



# Trajectory planning of abrasive belt grinding for aero-engine blade profile

Zhi Huang<sup>1</sup> · Rui Song<sup>1</sup> · Congbao Wan<sup>1</sup> · Pengxuan Wei<sup>1</sup> · Hongyan Wang<sup>1</sup>

Received: 30 May 2018 / Accepted: 11 December 2018 / Published online: 4 January 2019  
© Springer-Verlag London Ltd., part of Springer Nature 2019

## Abstract

In order to improve the efficiency and precision of abrasive belt grinding of the free-form surface, a novel trajectory planning approach based on machining accuracy control is proposed in this paper. At the same time, a method to optimize the size of the contact wheel based on the diploid genetic algorithm is also presented. Then, the effectiveness of the method is necessary to demonstrate through an abrasive belt grinding experiment of the aero-engine blade. The results show that the blade profile accuracy after grinding by using the proposed method can better meet the corresponding tolerance requirements, and the surface quality and accuracy of blade profile are improved effectively.

**Keywords** Abrasive belt grinding · Trajectory planning · Free-form surface · Error control

## 1 Introduction

The free-form surface products have delicate appearance, controllable shape, and excellent properties in aerodynamics, hydrodynamics, and thermodynamics, which have made it widely applied in aerospace, shipbuilding, automobile, energy, national defense, and other special industry products [1, 2]. The research on automatic grinding and polishing technology of the free-form surface in China is relatively lagging behind, and it is still mainly in the stage of the workpiece that is ground and polished by hand, which has low efficiency and high labor intensity. Unfortunately, the quality of the workpiece grinding and polishing often relies on the skill and experience of the workers [3, 4]. Because of that, the method of manual grinding and polishing failed to meet the processing requirements in aviation, shipbuilding, and other fields. Therefore, seeking an efficient grinding method of the free-form surface has become a research hotspot in the field of computer numerical control (CNC) machining. In the CNC machining process of the free-form surface,

the tool-path planning method has a direct impact on the machining accuracy and efficiency [5].

In the field of the abrasive belt grinding free-form surface, the maximization of the path interval in the processing can be achieved by optimizing the attitude angle of the contact wheel [6], which can effectively improve the machining efficiency. At present, many researchers have made lots of effort into theoretical research of abrasive belt grinding at moment.

Jourani et al. [7] presented a three-dimensional numerical model to study the contact between the belt constituted by abrasive grains and the surface. Huang et al. [8] put forward to a new measurement method of three-dimensional grinding force with mutual perpendicular and independent elastic elements which can effectively alleviate the inherent contradiction between the natural frequency and sensitivity in the traditional dynamometer. Hou et al. [9] proposed an effective method of the grinding surface based on the second-order osculation principle, which proved to be a practical machining method. Zhao et al. [10] studied the factors affecting the surface quality of the grinding parameters and optimized the grinding process parameters to improve surface quality. However, they did not consider the path change in the grinding process. Chaves-Jacob et al. [11] pointed out that optimizing the tool path can improve tool wear and surface coverage. Chen et al. [12] presented a novel method for tool-path generation to realize three-axis automatic

---

✉ Rui Song  
ruisonguestc@163.com

<sup>1</sup> School of Mechanical and Electrical Engineering, University of Electronic Science and Technology of China, Chengdu, China

machining of the free-form surface. Yang et al. [13] presented a path planning method of belt grinding for error region. However, this method was too complex to improve the processing efficiency. The error region and the magnitude of the error must be determined after the finish machining of aero-engine blades. Aiming at the problem of the unequal interval in space between the two adjacent lines in the equal parameter trajectory planning, He et al. [14] proposed an accurate overlapping method of the equal parameter path interval. Yang et al. [15] calculated the bandwidth of the whole cutting trajectory by using a second-order Taylor approximation, increasing the original cutting bandwidth by 26.5%. However, the calculation of the parameters is very difficult and the objects are studied by milling. At present, methods of trajectory planning commonly used in abrasive belt grinding and polishing are the iso-parametric method and equal residual high method. The trajectory of the tool generated by the iso-parametric method is relatively simple, but it is affected by the defined scallop height  $h$ , residual height, and the curvature of the free-form surface. Selected parameters of the tool path are more conservative and there is the redundant tool path. Though the optimal trajectory can theoretically be produced by the residual altitude method. The maximal distance calculation of the adjacent tool path is assumed to be in a plane, which means that the tangent vector direction of the adjacent tool-path trajectory is parallel. However, the fact is not that, and it is easy to cause a large deviation in the calculation of step distance for the curved surface. Due to the irregularity and constantly change the curvature of the free-form surface, it is very important to select the row spacing and step in the grinding process. If the size of the contact wheel is not selected correctly, the machining efficiency and machining precision will be directly affected. Therefore, it is very important to choose reasonable contact wheel size for free surface abrasive belt grinding. Current selection methods include empirical selection methods and curvature analysis methods [16]. The former chooses the tool size to be more conservative. The processing efficiency of the uncertainty is high, and it needs to repeatedly try to choose. The latter chooses the biggest tool size according to the result of surface curvature analysis. Compared to the experience selection method, the curvature analysis method is more scientific, but it is limited by the surface of discrete precision. It goes to save the calculation accuracy on the basis of the calculation time.

Aiming at the existing problems and shortcomings in the trajectory planning of free-form surface grinding, this paper studies the method of line processing, and proposes a new method which can optimize the size of the contact and the grinding parameters that of suitable for the surface machining process.

## 2 The optimal method for the optimal size of the contact wheel based on the genetic algorithm

### 2.1 Contact wheel size optimization standard and solution formula

Figure 1 shows a schematic diagram of abrasive belt grinding discussed in the paper. The principal curvature of the free-form surface determines the curvature radius of the surface. When machining the free-form surface, especially surface with a concave area, if the contact wheel radius is larger than the smallest curvature radius of the grinding point, local interference occurs, as shown in Fig. 2, which affects the processing quality and precision. In order to avoid interference, we must ensure that the contact wheel radius is less than the minimum principal curvature radius of the surface. Let  $\rho_{\max}$  be the maximum principal curvature radius of the surface, so the value of the contact wheel radius  $R$  should be less than  $1/\rho_{\max}$ .

Figure 3 shows two grinding methods for common aero-engine blades of the free-form surface. The contact area between the contact wheel and the surface is large in the horizontal spacing method and the grinding efficiency is high which is easy to produce the ripples along the length of the blade while the contact area between the contact wheel and the surface is small in the vertical spacing method and the machining accuracy is high and machining efficiency is low. In order to solve the problem of the low efficiency of the CNC machining of the free-form surface, this paper proposes a kind of technical approach which can improve the machining efficiency and satisfy the machining accuracy at the same time. This method is based on the error precision control principle to select the size of the contact wheel and the machining parameters. As shown in Fig. 4,  $AD$  is the width of the contact wheel and its value is  $W$ . The radius of curvature of the grinding point in the direction of the contact wheel is  $R_c$ . The gap

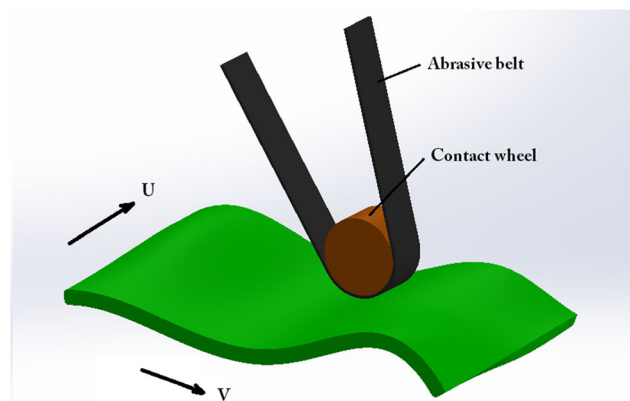


Fig. 1 Abrasive belt grinding

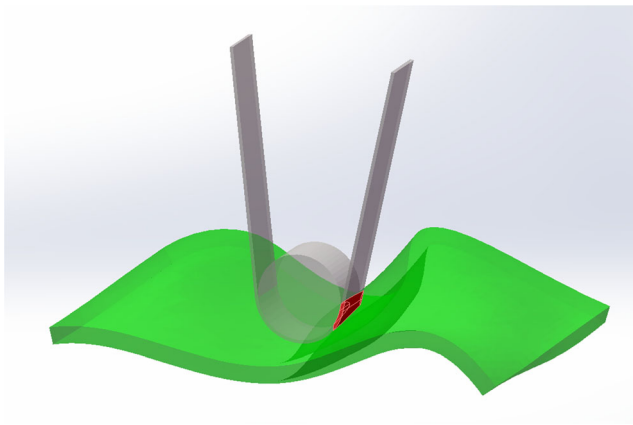


Fig. 2 Local interference

between the contact wheel and the surface is  $\varepsilon$ , and the machining allowance is  $h$ .

The gap between the contact wheel and the surface should satisfy Eq. (1).

$$\varepsilon \leq h \leq R_c - \sqrt{R_c^2 - (W/2)^2} \tag{1}$$

In order that avoid the gap between the contact wheel and the curved surface is greater than the expected machining allowance, the width of the contact wheel should satisfy Eq. (2).

$$W \leq 2\sqrt{2\varepsilon \cdot R_{cmin} - \varepsilon^2} \tag{2}$$

Where the radius  $R_{cmin}$  is the minimum radius of curvature of all grinding points in the direction of the contact wheel.

### 2.2 The maximum and minimum principal curvature of a surface by the genetic algorithm

According to Eq. (2), the problem of solving the size of the contact wheel can be transformed to find the maximum principal curvature of the free-form surface and the maximum principal curvature of all grinding points in the axial direction

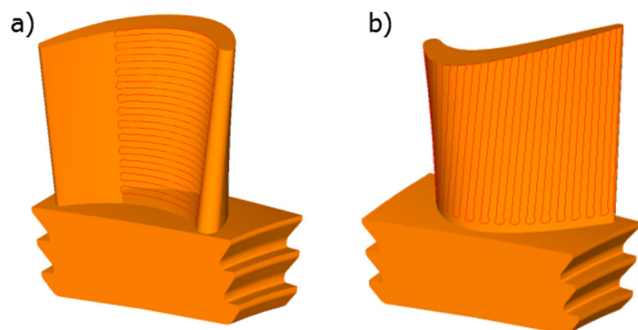


Fig. 3 Grinding manners. a Transverse processing. b Longitudinal processing

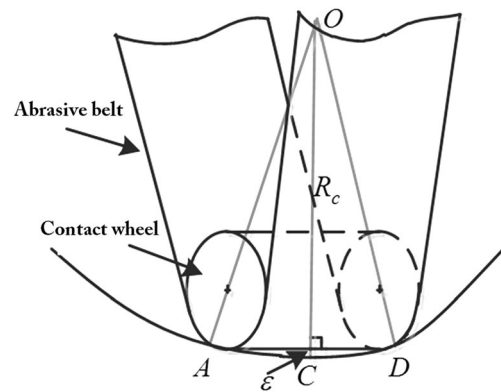


Fig. 4 Machining error along the axial direction

of the contact wheel. In order to maximum the width of contact area between the contact wheel and the surface during the grinding, the contact axis should always follow the first principal curvature direction of grinding point, so we only need to know the maximum principal curvature of the free-form surface and the maximum principal curvature in the first principal curvature direction [17]. The problem of finding the optimal solution in a typical group is how to find the main curvature parameters in the knife site quickly and accurately. Considering that the free-form surface includes two parameters  $u$  and  $v$ , this paper proposes a new algorithm to solve the problem of the solution of the maximum principal on the free-form surface and the first principal direction of the curvature surface based on the double genetic algorithm.

Assume that the function of the free form is  $S(u, v)$ .

$$S(u, v) = \begin{bmatrix} x(u, v) \\ y(u, v) \\ z(u, v) \end{bmatrix} \quad u, v \in [0, 1] \tag{3}$$

Where  $u, v$  is the parameters of the free-form surface. The three components  $x, y$ , and  $z$  are the two element differentiable functions of the parameters  $u$  and  $v$ . When  $u$  and  $v$  change continuously within a defined domain, it forms a surface with its corresponding points  $(x, y, z)$ . According to the solving formula of differential geometry, the normal curvature of the point on the free surface is as follows:

$$k_n = \frac{Ld_u^2 + 2Md_ud_v + Nd_v^2}{Ed_u^2 + 2Fd_ud_v + Gd_v^2} \tag{4}$$

In Eq. (4),  $E = S_u \cdot S_u, F = S_u \cdot S_v$ , and  $G = S_v \cdot S_v$  are the first kind of basic quantity of the surface.  $L = n \cdot S_{uu}, M = n \cdot S_{uv}$ , and  $N = n \cdot S_{vv}$  are the second kind of basic quantity of the surface. And  $S_u, S_v, S_{uu}, S_{uv}$ , and  $S_{vv}$  represent the first- or two-order partial derivatives.  $n$  represents the unit normal vector at the grinding point.

$$n = \frac{S_u \times S_v}{|S_u \times S_v|} \tag{5}$$

The principal curvature of the point on a free surface is the maximum and minimum of the normal curvature. According to the Gauss curvature and the mean curvature, the maximum and minimum principal curvature can be obtained as follows:

$$k_{1,2} = H \pm \sqrt{H^2 - K} \tag{6}$$

where  $H$  is the mean curvature and  $K$  is the Gauss curvature of the surface at arbitrary point  $P$ . From the above formula, we know that the main curvature  $K$  is a function of parameters  $u$  and  $v$ , and it needs to be considered at the same time.  $u$  and  $v$  are encoded by binary coding, and one of the individuals in the population is established together. Because the genetic algorithm is similar to the algorithm of solving the maximum principal curvature and the maximum principal curvature in the first principal curvature direction in the free-form surface, this paper explains the algorithm of the maximum principal curvature on the free surface.

Figure 5 shows the algorithm flowchart presented in this paper. The fitness function and the specific algorithms are described as follows:

Fitness function:

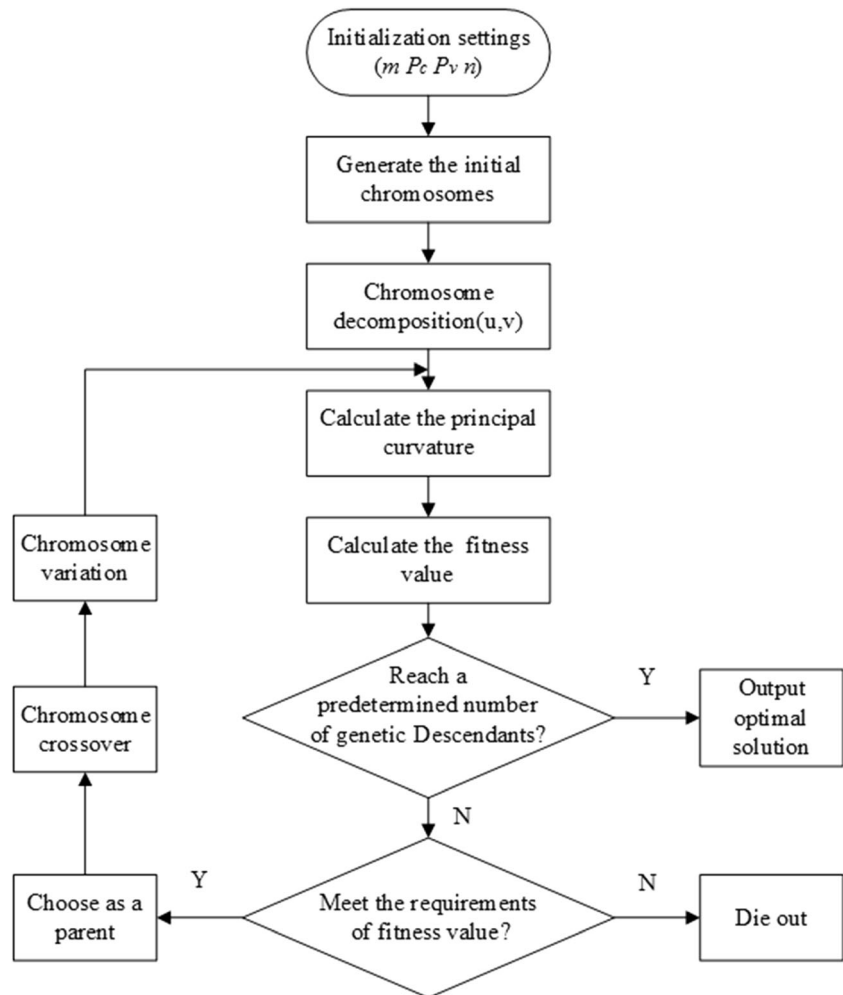
$$P(x_i) = \begin{cases} 1 - 0.5 \times \left( \frac{k_{\max} - k}{k_{\max} - k_{\chi}} \right)^{0.5} & k > k_{\chi} \\ \frac{1}{1 + \left( \frac{k_{\max} - k}{k_{\max} - k_{\chi}} \right)^2} & k \leq k_{\chi} \end{cases} \tag{7}$$

In Eq. (7),  $k_{\chi} = (1 - \chi) \times k_{\min} + \chi k_{\max}$ ,  $k$ ,  $k_{\max}$ , and  $k_{\min}$  represent the principal curvature calculated by the present individual, the maximum and minimum principal curvature of the population respectively.  $\chi$  is the adjustment coefficient and its value is 0.5 in this paper. The fitness function satisfies the non-negative and single value continuity requirements of the genetic algorithm and has the dynamic adjustment ability with the evolutionary process.

The descriptions of the genetic algorithm are as follows:

- Step 1. Set the number of the initial population is  $m$  and the number of the digits of binary code

Fig. 5 The flowchart of the genetic algorithm



which represents the length of the gene is  $n$ . The 8-bit binary is illustrated here as an example.  $P_c$  is the cross probability and  $P_v$  is the mutation probability. Binary code is generated randomly to represent the individual of a population, in which the binary code number is insufficient with 0 in the front.

- Step 2. Decompose the individual's binary code into a single chromosome on the parameters  $u$  and  $v$ , and calculate the actual parameter values of  $u$  and  $v$ . According to the above Eq. (5), the value of main curvature can be calculated. The fitness value of the principal curvature of the individual is obtained as the evaluation index in Eq. (7), and the roulette wheel method is used to eliminate the individuals who are not satisfied with the presupposition fitness.
- Step 3. According to fitness function, individuals with higher fitness function should be selected based on the probability of the roulette wheel method to enter the next generation. Among them, the individual 00000000 and the boundary individual 11111111 of the maximum value of the fitness function in the present age directly enter the generation.
- Step 4. The crossover and mutation operation of the new generation population is carried out according to the crossover probability  $P_c$  and the mutation probability  $P_v$ .
- Step 5. Recalculation of principal curvature according to a new generation of the population
- Step 6. Repeat steps (2) to (5) until the genetic algorithm ends and record the maximum principal curvature value  $k$  of the output and the corresponding parameters  $u$  and  $v$ .

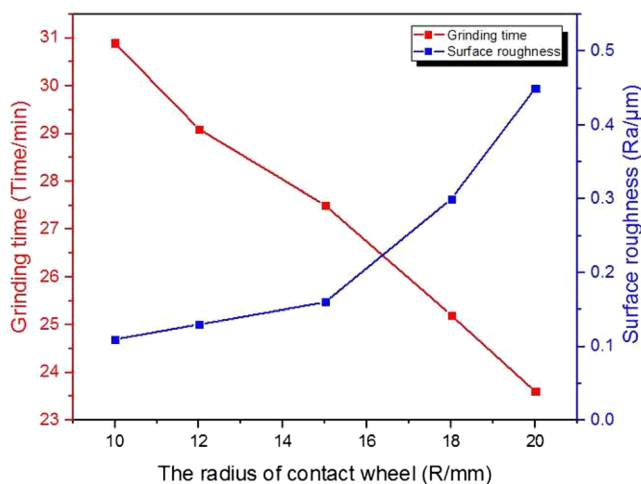


Fig. 6 An experimental curve of five contact wheels with different radii grinding the blade profile

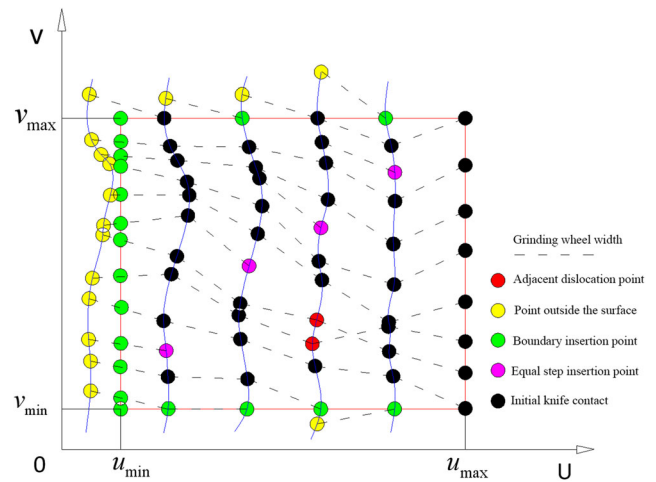


Fig. 7 Adaptive trajectory planning

### 2.3 The contact wheel size selection of non-interference efficient wide line machining

Through the above algorithm, we can get the maximum principal curvature  $k_m(u_m, v_m)$  on the free-form surface, and the principal curvature radius  $R_{cmin}$  of the first principal curvature can determine the minimum principal curvature radius of the surface.

$$R_m = 1/k_m \tag{8}$$

The width of wheel width:

$$W \leq 2\sqrt{2h \cdot R_{cmin} - h^2} \tag{9}$$

$R_m$  should be less than or equal to the standard contact wheel foot radius and  $W$  should be less than or equal to the standard width of the contact wheel. Based on the proposed algorithm, the contact wheel radius of an aero-engine blade grinding is calculated as  $R = 14.8$  mm (here we take  $R = 15$  mm) and  $W = 8$  mm. In order to verify the effectiveness of the proposed algorithm, five grinding experiments were carried out. Figure 6 shows the relationship between five contact wheels with different radii and grinding time and surface roughness under the same grinding condition. It can be seen that with the increase of the contact wheel radius, the grinding efficiency is gradually improved, but the surface quality after grinding is gradually reduced. Especially, when the size of the

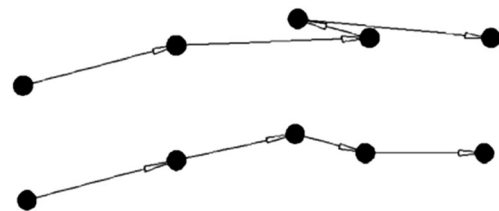


Fig. 8 The flexible adaptive processing effect diagram

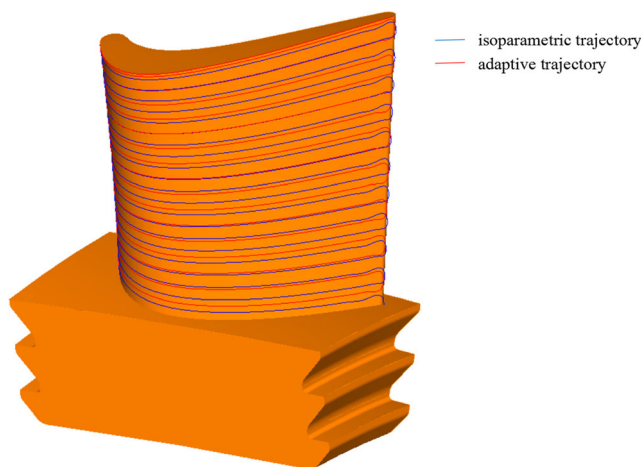


Fig. 9 Renderings of two kinds of trajectory planning

contact wheel is larger than the maximum radius of curvature of blade profile, the surface quality drops sharply, which is caused by local interference during the grinding process. Considering the machining quality and efficiency, the size of the contact wheel obtained by the proposed algorithm can avoid local interference in the grinding process and improve the machining efficiency and accuracy effectively.

### 3 The adaptive wide line trajectory planning algorithm

The ordinary iso-parametric line trajectory planning method turns into a curve because of its straight-line transformation in the parameter domain to Euclidean geometry space. The adjacent two equal parameter line paths with fixed parameter intervals are not equidistant in space [18]. Therefore, there is a need for a certain overlap between adjacent tracks in the wide line processing. However, it is still a technical problem in the field of precision CNC programming that how to determine the row spacing to ensure that the minimum overlap of two rows of adjacent cutter rails close to zero is still close to zero. Aiming at the problem of the minimum overlap between

adjacent knife and rail and the self-characteristics of transverse and wide line grinding, by effectively calculating the distance from each grinding point on the first principal curvature direction to the machining distance, and as the grinding point of adjacent track, the grinding points can be adaptive to the contact wheel axis. Moreover, it can also avoid the problem of solving the minimum lap in the wide line processing, and ensure the stability of the row spacing between the adjacent knife and rail.

#### 3.1 Calculation of adjacent grinding points

Take the width of the contact wheel  $W$  as the grinding distance of the grinding process. From the foregoing description, we can see that the nearest grinding point of grinding point is the distance from  $W$  to the first principal curvature direction. When the known surface function is  $S(u, v)$ , the current grinding point is  $C_{i,j}(u_i, v_j)$ .  $P_1$  is the direction vector of the first principal curvature direction.  $P_2$  is the direction vector of the second principal curvature direction.  $u$  and  $v$  are the parameter increments of two grinding points. The derivation of the parameters of the adjacent grinding points is as follows:

Because the first principal curvature direction vector is perpendicular to the second principal curvature direction vector, so

$$P_1 \cdot P_2 = 0 \tag{10}$$

It is also known that the vector formed by the current grinding point and the adjacent grinding point is along the direction of the first principal curvature and its distance is  $R_s$  that is the width of the contact wheel.

$$\begin{cases} \overrightarrow{C_{i,j}C_{i+1,j}} \cdot P_1 = W \\ \overrightarrow{C_{i,j}C_{i+1,j}} \cdot P_2 = 0 \end{cases} \tag{11}$$

The Taylor formula is used to expand the function  $C_{i+1,j}$  at  $C_{i,j}$  and omit the remainder of the two orders, which we can obtain the following:

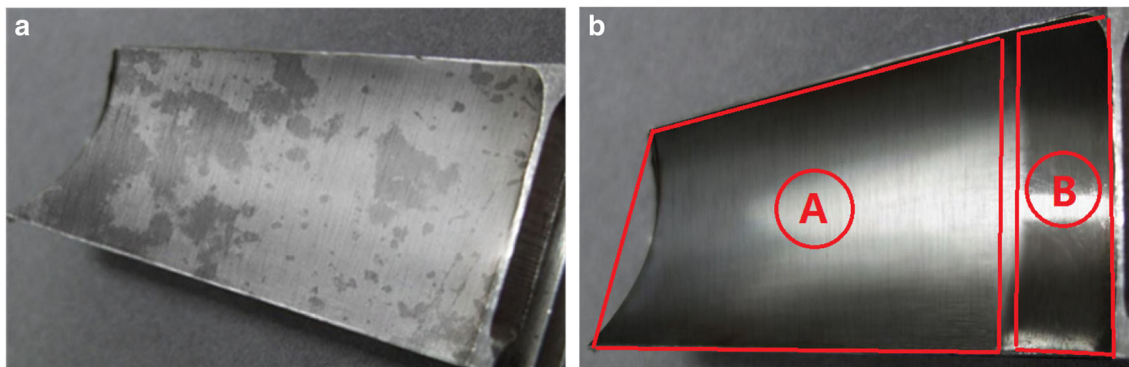


Fig. 10 Comparison of blade profile before and after grinding. a Before grinding. b After grinding

**Table 1** The error data before and after basin of blade grinding

	Detection area	minError/mm	maxError/mm	averError/mm	stdError/mm
Before processing	A	0.0129	0.0245	0.017	0.1401
	B	0.0131	0.0243	0.0172	0.1404
After processing	A	0.0066	0.0104	0.0086	0.0387
	B	0.0031	0.0053	0.0039	0.0172

$$C_{i+1,j} = C_{i,j} + S_u' \cdot \Delta u + S_v' \cdot \Delta v \tag{12}$$

$$\text{Set } T = -\frac{S_v' \cdot P_2}{S_u' \cdot P_2} \tag{13}$$

Simultaneous Eqs. (5), (6), (7), (8), and (9), we can obtain the following:

$$\Delta u = T \cdot \Delta v \tag{14}$$

$$\Delta v = \frac{W}{T \cdot S_u' \cdot P_1 + S_v' \cdot P_1} \tag{15}$$

According to Eqs. (10) and (11), the relation between adjacent grinding points can be obtained:

$$\begin{cases} u_{i+1} = u_i + \Delta u \\ v_{j+1} = v_j + \Delta v \end{cases} \tag{16}$$

the grinding point, and a grinding point in its first curvature direction distance spacing within the scope of the intersection, the situation is easy to cause the processing head reciprocating machining vibrations caused by processing vibration grain defects. So, in this paper, a flexible adaptive processing planning method is proposed to exchange the parameter information of the adjacent grinding points to realize the grinding point trajectory. The effect diagram is shown in Fig. 8. The idea is to traverse all new grinding points, remove the grinding point located outside the boundary, and insert the new boundary points. The grinding points in the different trajectories are traversed and the accuracy of the step size is calculated between the adjacent grinding points. The grinding points in the recent trajectories are traversed and the distance between adjacent grinding points is calculated. If the distance does not meet the requirement of step accuracy, a dichotomous interpolation is used to update the grinding point sequence until all adjacent grinding points meet the requirements of the step size.

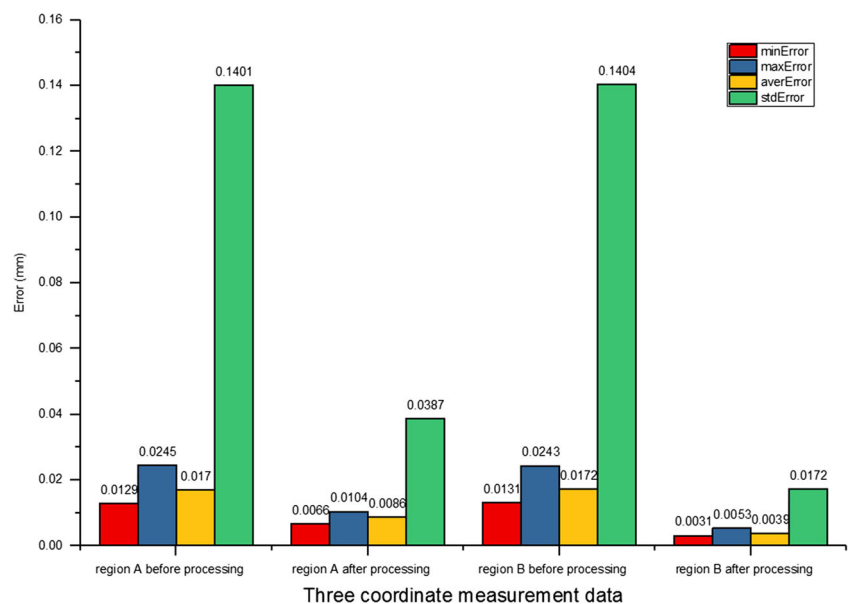
### 3.2 Flexible adaptive processing of grinding point trajectory

As shown in Fig. 7, a schematic diagram of the trajectory planning proposed in this article is presented. Because of the existence of some characteristics of the twisted blade surface,

### 3.3 Generating steps of the adaptive grinding path

The main steps of the adaptive grinding path planning for the free surface are as follows:

**Fig. 11** The error data before and after basin of blade grinding



- (1) First, the complex surface model is identified by feature recognition, and the long boundary line in the complex surface is selected as the initial track line of the tool. Then, according to the minimum step length principle, the grinding point is discredited by the dichotomous method.
- (2) Calculate the adjacent grinding points of the initial grinding point in the direction of the first main curvature.
- (3) Flexibility and interpolation for newly obtained grinding points
- (4) Repeat step (2) and step (3) until the grinding point covers the whole surface, and converts the track of the grinding point to the locus of the knife site.

Figure 9 is a comparison diagram of processing a single surface model of the aero-engine blade applied the method

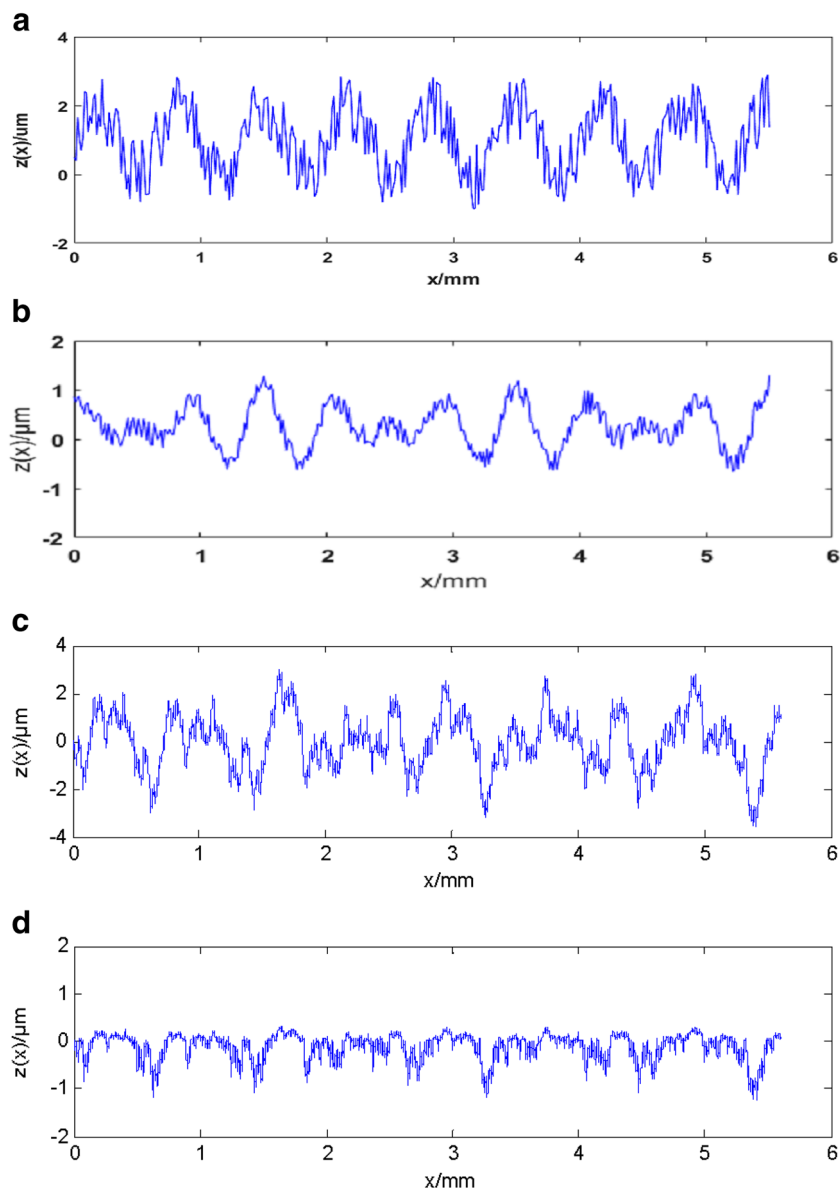
presented in this paper and an equal parameter trajectory planning method.

By contrast, we can intuitively find that the path generated by the method of line distance adaptive trajectory planning presented in this paper is always changing along the principal curvature direction of grinding point on the surface which effectively guarantee the best fit between the grinding head and workpiece, and at the same time, it also solves the problem of unequal space on the adjacent trajectories of equal parameters.

## 4 Experimental

The adaptive trajectory planning method proposed in this paper is verified by the experiment of processing the basin of an

**Fig. 12** Blade surface roughness before and after grinding. **a** The roughness of a sampling point in region A before grinding. **b** The roughness of a corresponding sampling point in region A after grinding. **c** The roughness of a sampling point in region B before grinding. **d** The roughness of a corresponding sampling point in region B after grinding





aero-blade on the CNC abrasive belt grinder (MTS1000-400-6NC). At the same time, we also conduct a grinding experiment on iso-parametric trajectory planning of the aero-blade. As shown in Fig. 10, region *A* is processed with iso-parametric trajectory planning while region *B* is processed with adaptive trajectory planning. Considering the practical application and processing efficiency of the engineering and the flexible contact of the sand belt itself, the radius and width of the contact wheel are properly amplified. The radius of the contact wheel is 15 mm and the width is 8 mm. The belt speed is 12 m/s. The abrasive grain is 280<sup>#</sup> and the tolerance is 3.0  $\mu\text{m}$ .

## 5 Results and discussion

As shown in Fig. 10, the comparison of the whole shape of the blade before and after the grinding process shows that the machining surface is smooth without any defects such as curvature interference, and the machining quality is good. We also find that region *B* has better gloss than region *A*. In the grinding process, the adaptive trajectory planning automatically adjusts the processing step length according to the curvature of the processed surface, making the surface smoother after machining than iso-parametric trajectory planning.

The measurement data is measured using hexagon global series three coordinate-measuring machines. After data processing, as shown in Table 1, the error data before and after basin of blade processing are obtained from the blade surface.

Figure 11 clearly shows the error data before and after basin of blade processing. Through comparative analysis, it was found that the minimum surface error of region *A* was reduced from 0.0129 to 0.0066 mm, and the error reduced by 48.8%. The maximum error was reduced from 0.0245 to 0.0104 mm, and the error reduced by 57.6%. The average error decreased from 0.017 to 0.0086 mm, which decreased by 49.4%, and the standard error decreased from 0.1401 to 0.0387 mm, which decreased by 72.4%. The minimum surface error of region *B* was reduced from 0.0131 to 0.0031 mm, with a decrease of 76.3%; the maximum error was reduced from 0.0243 to 0.0053 mm, with a decrease of 78.2%; the average error was reduced from 0.0172 to 0.0039 mm, with a decrease of 77.3%; and the standard error was reduced from 0.1404 to 0.0172 mm, with a decrease of 87.7%. According to the above error comparison, it can be clearly found that the machining error through adaptive trajectory planning is significantly smaller than that of iso-parameter trajectory planning.

The Marsurf roughness profilometer was used to detect the surface roughness of area *A* and area *B* before and after machining. As shown in Fig. 12, it can be seen that the roughness of the surface which is processed has been greatly improved. The reason is that the complex interaction between abrasive belt and a metal layer on the surface of the workpiece can smooth the original bump on the surface of the workpiece.

As a result, the roughness profile is smaller and more uniform, so the roughness of the machined surface is effectively reduced, and the surface quality of the blade surface after grinding is greatly improved compared with that before processing.

## 6 Conclusion

In this paper, an adaptive trajectory planning approach of abrasive belt grinding for the aero-engine blade is presented. The presented method analyzes the relationship between the width of the contact wheel and the curvature of the surface which avoid the interference between them. The conclusions can be drawn as follows:

- (1) When using the diploid genetic algorithm to optimize the size of the contact wheel, local interference can be effectively avoided in the grinding process.
- (2) The best fit of the contact wheel and the workpiece is realized by controlling the posture of the contact wheel during the processing cycle and the optimum grinding effect is achieved by adaptive trajectory planning based on error control for grinding point.
- (3) Compared with the iso-parametric trajectory planning, the adaptive trajectory planning proposed in this paper has higher precision and efficiency in blade grinding.

**Funding information** This work was financially supported by the National Natural Science Foundation of China (grant number 51275078).

**Publisher's note** Springer Nature remains neutral with regard to jurisdictional claims in published maps and institutional affiliations.

## References

1. Wu BH, Luo M, Zhang Y, Li S, Zhang DS (2008) Advances in tool path planning techniques for 5-axis machining of sculptured surfaces. *Chin J Mech Eng* 44(10):9–18
2. Zhou ZX, Ren YH (2010) Current research and development trends of complex surface machining technology. *J Mech Eng* 46(17):105
3. Ng TJ, Lin WJ, Chen XQ, Gong ZM, Zhang JB (2004) Intelligent system for turbine blade overhaul using robust profile reconstruction algorithm. 8th International Conference on Control, Automation, Robotics and Vision, December 6-9, 2004, Kunming, China. IEEE, New York, pp 178–183
4. Zhao HH, Wang Y (2007) Development and actuality of grinding process. *Manuf Technol Mach Tool* 2:39–41
5. Xu JT, Liu XR (2010) Isoparametric and spiral toolpath for free-form surfaces machining. *J Mech Eng* 46(03):148–154
6. Chen ZT, Yue (2011) A middle-point-error-control method in strip-width maximization-machining. *J Mech Eng* 47(1):117–123
7. Jourani A, Dursapt M, Hamdi H, Rech J, Zahouani H (2005) Effect of the belt grinding on the surface texture: modeling of the contact and abrasive wear. *Wear* 259(7–12):1137–1143
8. Huang Z, Chen SH, Wang HY (2016) Development of three-dimensional dynamic grinding force measurement platform, ARCHIVE Proceedings of the Institution of Mechanical

- Engineers Part C Journal of Mechanical Engineering Science, 203-210:1989–1996
9. Hou B, Wang YQ, Wang FB, Ji ZC, Liu HB (2015) Research on belt grinding for marine propeller blade based on the second-order osculation. *Int J Adv Manuf Technol* 80(9–12):1855–1862
  10. Zhao T, Shi YY, Lin XJ, Duan JH, Sun PC, Zhang J (2014) Surface roughness prediction and parameters optimization in grinding and polishing process for IBR of aero-engine. *Int J Adv Manuf Technol* 74(5–8):653–663
  11. Chaves-Jacob J, Linares JM, Sprauel JM (2013) Improving tool wear and surface covering in polishing via toolpath optimization. *J Mater Process Technol* 2013(10):1661–1668
  12. Chen T, Shi ZL (2008) A tool path generation strategy for three-axis ball-end milling of free-form surfaces. *J Mater Process Technol* 208(1):259–263
  13. Yang JH, Zhang DH, Wu BH, Zhang Y, Luo M (2015) A path planning method for error region grinding of aero-engine blades with free-form surface. *Int J Adv Manuf Technol* 81(1–4):717–728
  14. He Y, Chen, ZT, Wu XZ (2014) Iso-parametric tool path overlapping method for sculptured surfaces in wide strip machining. *Acta Aeronautica et Astronautica Sinica* 35(4):1142–1148
  15. Yang JH, Zhang DH, Zhang J, Wu BH (2013) An approach to strip-maximization machining based on tolerance constraints for sculptured surfaces. *J Mech Eng* 49(3):130
  16. Li HY, Zhang YF (2009) Automatic tool-path generation in 5-axis finish cut with multiple cutters, *IEEE International Conference on Virtual Environments, Human-Computer Interfaces and Measurements Systems*, pp 210–213
  17. Chiou C, Lee Y (2002) A machining potential field approach to tool path generation for multi-axis sculptured surface machining. *Comput Aided Des* 34(5):257–371
  18. Lasemi A, Xue D, Gu P (2010) Recent development in CNC machining of freeform surfaces: a state-of-the-art review. *Comput Aided Des* 42(7):641–654